Journal of Pharmacy & Allied Medicine

JPAM, 3(2), 62-73, 2025
https://doi.org/10.58985/jpam.2025.v03i02.33
ISSN (Print): 3005-2726

Research Article

Formulation and evaluation of trametinib loaded novel nano elastic carriers for treatment of melanoma

Chokkarapu Suryanarayana[1], Ankit Singh[1] and **Ananda Kumar Chettupalli[2*]**

1. Department of Pharmaceutical sciences, Shri Jagdish Prasad Jhabarmal Tibrewala University Chudela Jhunjhunu Rajasthan- 333001, India.
2. Department of Pharmaceutical sciences, School of Medical and Allied Sciences, Galgotias University, Greater Noida, UP-203201, India.

Article Information
Received: 18 December 2024
Revised: 07 March 2025
Accepted: 11 March 2025
Published: 11 June 2025

Academic Editor
Prof. Dr. Christian Celia

Corresponding Author
Prof. Dr. Ananda Kumar Chettupalli
E-mail: anandphd88@gmail.com
Tell: +91-9849922424

Keywords
Bilosomes, anti-oxidant, melanoma, tracmetinib.

Abstract

For the treatment of resistant cancers characterized by BRAF-V600E gene mutations, such as melanoma and advanced lung adenocarcinoma, the FDA has granted a license for trasmetinib (TM), a targeted therapeutic. Inhibiting mitogen-activated extracellular signal-regulatory kinase (ERK) is key to its efficacy. However, commercial TM is poorly soluble, cannot target certain biological targets, and most worrisomely, it is easy to induce tumor cells to develop resistance to many medications, therefore, it has limited practical medical applications. We formulated TM-BLs, which are bilosomes that contain TM, and evaluated their entrapment efficiency, zeta-potential, and vesicle size. The formulations including cholesterol, sodium deoxycholate (SDC), and Tween 80 were used for thin film hydration. The formulations coated with the high concentrations of the mucoadhesive polymer chitosan (0.5 and 1% w/v) performed the best. Surface morphological, anti-oxidant, and antibacterial tests were conducted on the bilosomes coated with chitosan (TM-CBLs). For BS3, the synthesized TM-BLs had a nanometric size of 185.34 ± 5.28 nm, whereas for BS5, it was 295.31 ± 6.31 nm. In addition, their electrical conductivity increased, from 56.49 ± 0.16 to 80.27 ± 0.64%, and they possessed a negative zeta potential of -10.74 ± 1.06 and -21.54 ± 1.42 mV. Their polydispersibility index was also less than 0.5. These findings led to the subsequent coating of the selected formulation (BS2) with chitosan. The end outcome was an increase in vesicle size (268.49 ± 2.31nm), a positive zeta potential (17.36 ± 0.52 mV), and an enhancement in drug release (69.37 ± 1.34%). Because, chitosan is a polymer that adhears to mucous membranes, TM-CBLs formulation showed significantly better permeability and mucoadhesion ($p < 0.05$) than the formulation BS2. When chitosan is bound to BL surfaces, it opens previously impermeable tight membrane junctions, allowing for increased permeability. The vesicles were clear and unaggregated, as confirmed by scanning electron microscopy results. TM-BLs and TM-CBLs showed significantly higher antioxidant activity compared to pure TM. Bile salt and chitosan coating improved solubility and enhanced radical scavenging effects. The zones of inhibition for antibacterial and anti-oxidant activities demonstrated better outcomes. This study suggests that TM-BLs can impede the success of traditional distribution techniques.

1. Introduction

Bilosomes incorporate bile salts into their membranes and are novel vesicular nanocarriers. These nano-vesicular carrier systems outperform alternatives in terms of flexibility, elasticity, and ultradeformability.

This article is an open access article distributed under the terms and conditions of the Creative Commons Attribution 4.0 International License (CC BY-NC 4.0).

Liposomes and niosomes are two examples of conventional nanovesicular carriers that can protect drugs from enzymatic breakdown in the gastrointestinal tract (GIT). [1, 2] When intestinal bile salts are present in the GIT, these carriers fail, releasing the encapsulated molecule before it reaches its target [3, 4]. To overcome the issues associated with standard nano-vesicular carrier systems, stable bilosomes are created by adding bile salts to their lipid bilayers. Their design protects them from bile salts in the intestines and GIT, which increases their stability. Bile salts increase the oral bioavailability of low-water-solubility and intestinal-permeability medicines [5]. Scientists employ bile salts (like sodium glycocholate: SGC, SDC, STC, Sodium Taurocholate: STC, and others) to stabilize nano-vesicular carrier systems in the gastrointestinal tract. Due to its reduced toxicity, improved penetration impact, and increased protease enzyme-inhibiting capacity in the GI tract, SGC is one of the most favored options [6, 7].

Non-ionic surfactants are widely used as surface-active agents to formulate bilosomes due to benefits such as stability, compatibility, and low toxicity compared to other types of surfactants [8]. The formation of micelles or bilayer vesicles depends on the surfactant's hydrophile-lipophile balance (HLB), component chemical structure, and crucial packing parameter (CPP) [9]. Surfactants of the span and tween classes feature long alkyl chains and wide hydrophilic groups, which have a shorter alkyl chains, and can entrap water-soluble medications more effectively when mixed with cholesterol in a 1:1 ratio [10].

Bilosomes are biocompatible because they contain natural lipids like cholesterol. Cholesterol often affects bilosome properties, including toxicity, rehydration ease after freeze-drying, encapsulation efficiency, membrane permeability, and stiffness, particularly when mixed with other forms of cholesterol. They are useful for hydrophobic and hydrophilic medications, vaccines, therapeutic proteins/peptides, and oral delivery [11].

Melanoma, potentially fatal cancer can develop from the melanocytes in the skin. According to Swaika et al. [12]. This fatal form of cancer accounts for around 4-6% of all cancer cases. Melanomas have increased over 30 years. From 2001 to 2022, the data showed a 53% increase in the number of newly diagnosed melanoma cases.

The FDA has approved the clinically targeted medication trametinib (TM), which inhibits mitogen-activated extracellular signal-regulatory kinase (ERK), as a treatment for resistant malignancies with BRAF-V600E gene mutations, including melanoma and advanced lung adenocarcinoma [13]. However, the commercial Tr is limited in clinical applications because of its low solubility, lack of bio-targeting and the more serious fact that it easily induces multi-drug resistance tumor cell [14]. Some nanoparticle-mediated tumor treatments have been proposed to enhance the therapeutic efficacy of Tr. These include inorganic nanoparticles [15]. polymeric micelles [16]. nanoformulations of small molecule medications [17]. etc. Due to their biodegradability, low toxicity, and moderate immunogenicity, nano-scale bilosomes are the most promising. Furthermore, there has been encouraging research into nanoparticle-based drug delivery methods to avoid the P-glycoprotein (P-gp) transport of anti-tumor drugs, which might address the issue of TM drug resistance. The development of nanobilosomes for the treatment of TM-resistant melanoma is challenging.

The lengthy production process of this method makes it difficult to scale up, and orally administered self-emulsifying nanoemulsions enhance bioavailability [18]. Thus, bile salt-containing vesicles would improve GIT absorption and eliminate the issues associated with oral TM administration. Although liposomes and niosomes can protect TM from degradation in the gastrointestinal system, bilosomes restrict membrane distortion and vesicle lysis, releasing TM at its target location [19-21]. Thin film hydration TM-BS formulations were examined for optimal particle size, low polydispersity index, drug entrapment, dissolving rate, and bioavailability. We tested our theory. Bile salt (sodium glycocholate) in the bilosome formulation enhanced TM permeability, improving pharmacokinetics, histology and resistance to bile salt disruption in the GIT.

The highly futuristic bilosome has an extremely innovative nano-elasticity, deriving its identity from its unique structural constitution and functional advantages as a new drug delivery vehicle. The

https://doi.org/10.58985/jpam.2025.v03i02.33

bilayer membranes of these vesicles incorporate bile salts conferring flexibility, deformability, and instability against gastrointestinal degradation. The bilosomes are much more resistant than liposomes and niosomes against rupture of the membranes caused by bile salts, thus enhancing drug stabilization and bioavailability, particularly in the oral and transdermal routes of administration. Due to their nanosize, further enhancement of permeability, targeting, and drug release may be facilitated. This imparts characteristics that characterize bilosomes as a novel and, hopefully, an advance in enhanced drug delivery technology.

1.1. Unique properties of nano-elastic carriers in advanced drug delivery

Nano-elastic carriers, such as bilosomes, possess several unique properties that distinguish them in the field of advanced drug delivery systems:

1. *High deformability & elasticity* – Their flexible structure allows them to pass through biological barriers more effectively than conventional liposomes and niosomes.
2. *Improved bioavailability* – Their nanoscale size enhances cellular uptake and absorption, leading to better therapeutic outcomes.
3. *Stability against enzymatic degradation* – Bilosomes incorporate bile salts, which protect them from enzymatic degradation in the gastrointestinal tract, making them ideal for oral drug delivery.
4. *Controlled and sustained drug release* – Nano-elastic carriers can regulate drug release, ensuring prolonged therapeutic effects and reduced dosing frequency.
5. *Mucoadhesive properties* – Chitosan-coated bilosomes enhance drug retention at target sites by adhering to mucosal surfaces, improving permeability and absorption.

2. Materials and methods

2.1. Materials

The Hetero laboratory in Hyderabad, Telangana, India, provided TM as a gift SGC dried, extremely pure, M.W.487.60, and dialysis sac (MWCO: 12000 Da, average flat width was 2.5 mm, capacity of 60 mL/ft, 16 mm diameter) were purchased from Sigma Aldrich, India, and S.G Enterprises, New Delhi, India. Cholesterol was supplied by Thermo Fisher Scientific, through Indian firm Chloroform, Cremophor, span 60, tween 60, and diethyl ether were obtained from SD Fine Chemicals in Mumbai, India. SD Fine Chemicals in Mumbai, India, sold mannitol with a molecular weight of 182.17 g/mol. An analysis-grade set of chemicals and reagents were used in the investigation.

2.2. Preparation of TM loaded BLs

Waglewska et al. [22] proposed a thin film hydration process that was used to create BLs loaded with TM. In summary a round-bottom flask containing 10 mL of chloroform was ultrasonicated for 10 minutes (Model SH 150-41; USA) to dissolve 10 mg of TM, 7.5 mg of cholesterol (CH), 10 mg of bile salt, and 50 mg of surfactant. Rotary evaporation at 40 °C under reduced pressure for 30 minutes produced a dry, thin layer from the organic solution. After letting the evaporated film overnight to remove the organic solvents, it was rehydrated in 10 mL of distilled water with STC. The liquid was magnetically swirled for 2 h to create a TM-BL dispersion (Table 1). The particle size of the BLs was reduced by ultrasonicating them for 5 min (Bandelin, Berlin, Germany). Until usage, the TM-BLs dispersion was stored at 4°C [23].

2.3. Bilosomal optimization

Based on the goal, future studies should use small vesicles, low PDI, and high drug entrapment. We achieved this by investigating how various variables affected PDI, %EE, and particle size.

2.4. Physicochemical characterization

2.4.1. ZP, PDI, size of particles

The Brownian motions of nanocarriers with a light incidence angle of 173° were measured using Malvern Instruments' Zetasizer Nano Series software to determine the bilosome particle size. Three sets of ten measurements in disposable polystyrene cuvettes at 25 °C yielded Z-average (Z-Ave) and polydispersity index. We calculated the surface electric charge (ζ-potential) of the nanobilosomes using the Smoluchowski equation, electrophoretic mobility technique, and particle tracking in an electric field. At least twenty measurements were made in a folded capillary zeta cell using the same equipment at 25 °C from three runs. Z-Ave, PdI, and ζ-potential measurements were repeated to confirm system stability after 14 and 30 days at 4 °C [24].

https://doi.org/10.58985/jpam.2025.v03i02.33

Table 1. Formulation of drugs loaded Novel nano elastic vesicles (bilosomes)

Drug/Excipients	BS-1	BS-2	BS-3	BS-4	BS-5	BS-6	CBS-1	CBS-2
Trametinib (mg)	10	10	10	10	10	10	10	10
SDC (mg)	10	20	30				20	20
STC (mg)	-	-	-	10	20	30	-	-
Tween 80 (mg)	40	50	60				50	50
Cremophor EL(mg)	-	-	-	40	50	60	-	-
Cholesterol (mg)	7.5	15	30	7.5	15	30	15	15
Chloroform (mg)	10	10	10	10	10	10	10	10
Chitosan (%w/v)	-	-	-	-	-	-	0.5	1

2.5. Entrapment efficiency (%)

The use of the direct technique allowed for the estimation of entrapment efficiency. After a 10-minute sonication in ethanol, TM-BLs were filtered using a Millipore Co., USA Millex-LG syringe filter (pore size: 0.4 μm). Measured TM trapped in BLs using a Shimadzu UV spectrophotometer (2401/PC Japan) at 245 nm. Equation 1 calculates employment equity: Using the direct method, entrapment efficiency was estimated. After a 10-minute sonication in ethanol, TM-BLs were filtered using a Millipore Co., USA Millex-LG syringe filter (pore size: 0.4 μm). The amount of trapped TM was measured using a Shimadzu UV spectrophotometer (2401/PC Japan) at 245 nm [24, 25]. This is the equation (Equation 1) that was used to determine the employment equity percentage.

$$EE\ (\%) = \frac{\text{Amount of encapsulated drug}}{\text{Total amount of drug}} \times 100 \quad \text{Eq---(1)}$$

2.6. Scanning electron microscope

SEM was used to study optimal bilosomal formulations and they system forms. First, freshly prepared samples (1 mg/mL) were mixed with filtered deionized water (1:50) and sonicated for 5 min at room temperature. We used a carbon-coated copper grid to hold a drop of the sample after a 30-second staining in 1% uranyl acetate aqueous solution. A SEM (JEOL, Tokyo, Japan, JEM-2100F) was used to examine the stained film for further details [26].

2.7. In-vitro drug release and release kinetics

In vitro drug release was evaluated using the dialysis bag diffusion technique. A cellulose dialysis bag contained 10 mg of BLs dispersion and 15 cc of 0.1 M PBS (pH 6.8). An additional 0.1% tween 20 was added to maintain sink conditions. Keeping the volume and sink conditions constant, 2 mL receiver media samples were replaced with equal amounts of fresh medium at regular intervals. The amount of TM in the receiver media samples was measured using UV spectrophotometry at 245 nm [26, 27]. The release data from several BLs formulations, PIP suspensions, and CU were fitted to various equations using the DD solver tool, including zero-order, first-order, and Higuchi equations.

2.8. Antioxidant activity of TM and TM-BS

The DPPH radical scavenging technique was used, as described by [28]. TM and TM-BS stock solutions (1 mg/mL) were dissolved in methanol, followed by 10-150 μg/mL concentrations. When not in use, the 0.1 M DPPH solution was stored in methanol at 40°C. Each sample was mixed with 100 μL of DPPH solution and left in a dark room for 1 h to complete the reaction. The hue changed from violet to colorless when the reaction was completed indicating that the scavenging activity was successful. A UV-spectrophotometer set at 571 nm was used to assess the absorption. To ensure accuracy, a control solution known as butylated hydroxytoluene (BTH) was used. antioxidant activity of the sample was determined using the equationg Equation:

$$\text{Antioxidant activity (\%)} = \frac{\text{Abs Control} - \text{Abs of test sample}}{\text{Abs control}} \times 100 \quad \text{Eq---(2)}$$

2.9. Radical-scavenging ABTS

A slight variation from the previously stated strategy was used to conduct the investigation (Chaves et al., 2020) [29]. To prepare the ABTS solution, 0.1 mL of each dispersion was mixed with 3.9 mL of TM and TM-BS at 10 to 150 μg/mL, then vortexed. After 30 min of incubation in the dark, UV-Vis spectrophotometry

https://doi.org/10.58985/jpam.2025.v03i02.33

Table 2. Physicochemical characterization data of TM-BLs

Formulation code	VS (nm)	EE (%)	PDI	ZP (mV)	Drug Loading (%)
BS-1	256.34±3.46	76.54±0.35	0.135±0.01	-11.58±1.02	69.35±1.24
BS-2	213.85±6.91	80.27±0.64	0.169±0.04	-21.54±1.42	82.58±2.56
BS-3	185.34±5.28	65.34±0.28	0.218±0.03	-15.69±1.03	76.42±3.28
BS-4	287.41±4.72	56.49±0.16	0.312±0.05	-10.74±1.06	59.34±2.49
BS-5	295.31±6.31	62.57±0.53	0.279±0.01	-14.53±1.52	60.18±2.45
BS-6	264.58±5.34	70.31±0.28	0.326±0.06	-11.84±1.48	63.59±1.06
CBS-1	268.49±2.31	89.36±0.45	0.432±0.04	17.36±0.52	87.35±0.26
CBS-2	352.74±3.65	91.24±1.36	0.496±0.06	21.48±0.18	90.42±0.59

was performed at 734 nm [30]. Comparison control was a BTH solutions. The scavenging activity %, was calculated using the following formula.

$$\text{Antioxidant activity (\%)} = \frac{\text{Abs Control} - \text{Abs of test sample}}{\text{Abs control}} \times 100 \quad \text{Eq---(3)}$$

2.10. Antimicrobial study

A cub plate test was used to assess the bactericidal activities of pure TM and TM-BS against *Staphylococcus aureus* and *E. coli.* Colonies were grown in nutrient broth with 5x106 CFU/mL bacterial load. A autoclave (121^{0}C) was used to sterilize the nutritious agar medium. After transferring to a sterile Petri plate and solidifying under aseptic conditions, the 0.5 mL diluted microbial strain was mixed with the liquid nutritional agar medium. After curing, a sterile stainless-steel borer made 6-millimeter cups. The TM and TM-BS samples were put in separate cups and allowed to stand for two h to facilitate absorption [31]. Subsequently, the, petri dish was turned upside down and placed in an incubator set at 37^{0}C for a whole day. A graduated scale was used to evaluate the zone of inhibition (ZOI).

2.11. Statistical analysis

Experimental design software (Version 8.0.6) was used to optimize the formulation. values were represented as mean ± standard deviation. Statistical analyses were conducted using GraphPad, a program developed by InStat in California, USA. Data analysis included one-way analysis of variance and Tukey-Kramer multiple comparison tests. Substantial variations were considered when P < .05.

3. Results and discussion

TM-BLs were prepared by thin film hydration of cholesterol, SDC, and STC (Table 1). Primarily, BLs' negatively charged surface and cholesterol's positively charged surface produced TM-BLs by electrostatic interactions. Anionic BLs undergo size and zeta potential alterations upon the introduction of positively charged groups. The creation of double-layered vesicles and subsequent cholesterol coating on their surfaces may have contributed to their enlargement [32, 33]. The prepared TM-BLs were characterized by nanometric VS, low PDI, negative ZP, and high EE. These results informed the decision to coat the chosen formulation (BS2) with cholesterol at concentrations of 7.5 and 30 mg; further experiments showed a significant growth in size and the absence of a zeta potential.

3.1. Vesicle characterization

The evaluation of produced TM-BLs, VS, EE, PDI, drug loading, and zeta potential were presented in Table 2 and shown in Fig 1). It showed that TM-BLs had a significantly different VS ($p < 0.001$). TM-BLs exhibited mean diameters ranging from 185.34 ± 5.28 nm (BS3) to 295.31 ± 6.31 nm (BS5). The formulation with the smallest size, BS3, had a particle size of 185.34 ± 5.28 nm. Prior to coating with chitosan the size was 213.85 ± 6.91 nm, but after coating, it increased to 268.49 ± 3.02 nm, a significant increase ($p < 0.001$). There was a substantial ($p < 0.001$) effect of the chitosan concentration (0.5% or 1%) on the vesicle size. According to the literature, medications are transported by particles with a diameter less than 500 nm via the endocytosis route, whereas bigger particles are transported through the lymphatic system [34]. We found that the particle sizes of TM-BLs and TM-CBLs were less than 500 nm. A larger surface area is available, which can further improve the absorption

https://doi.org/10.58985/jpam.2025.v03i02.33

of medication. Within the ranges of 0.13 to 0.39, there was no discernible change in the PDI value. Based on their PDI values being less than 0.7, TM-BLs and TM-CBLs were deemed appropriate delivery methods [35]. Cellular contact and absorption are greatly impacted by the vesicle's surface charge. Prepared TM-BLs have a very high negative zeta potential, which indicating their high stability. Values between -10.74 ± 1.06 and -21.54 ± 1.42 mV were observed in the nano-sized TM-BLs, with ± 30 mV being deemed stable [36]. A defining feature of TM-BLs may be observed in these values. Its flocculation was more powerful than its repulsive forces. One possible explanation for the low ZP is the role of lipids, which produce negative charges in water [37]. The BLs were attracted to one another because the positively charged chitosan coated every surface of the particles [38]. Due to its positive charge, chitosan interacts readily with the negatively charged intestinal mucus, which enhances the drug's effects.

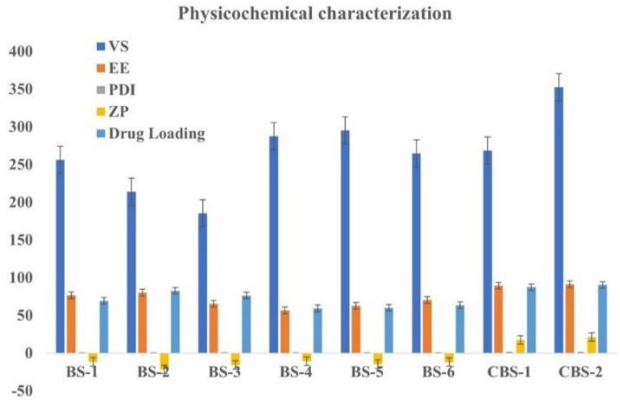

Figure 1. Physicochemical characterization data of TM-BLs.

3.2. Entrapment efficiency (EE)

The amount of TM trapped in the bilosomes, was evaluated (Table 2). Due to variations in the composition of BLs, there were notable variations in the EE, ranging from 56.49 ± 0.16 to 80.27 ± 0.64% ($p < 0.001$). The sample with the chemical composition of STC (10 mg) and cremophre EL (40 mg) had a minimum electrical conductivity (EE) of 56.49±0.16%. The encapsulation efficiency was highest (80.27 ± 0.64%) in formulation BS2 when SDC (10 mg) and tween 80 (50 mg) were. used. EE was shown to be more effective when the concentration of bile salts and surfactants was increased, rather than decreased. According to the findings, the EE was not substantially raised, either T80 or SDC on their own. In comparison to either T80 or SDC alone, the improved EE was considerably ($p < 0.05$) achieved by the 1:1 mixture of SDC and T80. Mixed micelles may be formed and improved solubility in the dispersion media may result from their use at high concentrations [39, 40]. The formulation (BS2) was coated with 0.5% and 1% chitosan. EE was not significantly different among the TM-CBLs (CBS-1 and CBS-2). A slight change in the EE was also detected between CBS-1 (89.36 ± 0.45%) and CBS-2 (91.24 ± 1.36%). To prevent the leakage of the medication from the liposomes, chitosan was coated on their surfaces [41]. The somewhat elevated EE was ovserved in the CBS-2 formulation, attributed to the high chitosan (1%) content of the coated polymer. Lipid and polymer concentrations determine the efficacy of the encapsulated medication. Entrapping hydrophobic medications in a lipid bilayer is a simple process.

3.3. SEM evaluation

The ready-made TM-BLs (optimized BS2) and TM-CBLs (CBS-1) exhibited non-aggregated spherical shapes on their surfaces (Fig. 2). A thin covering was obsrved and the surface appeared smooth. Size distribution curve analysis was also performed on samples (BS2, CBS-1) and the results demonstrated a range of sizes from 200 to 45 nm. The distribution histograms consistently confirmed the SEM particle size picture [42].

3.4. Drug release (%)

An analysis of the drug release of TM-CBLs, TM-BLs, and pure TM are shown in Fig. 3. Data from in vitro release experiments showed that both TM-BLs (BS2) and TM-CBLs (CBS-1) released more TM. The findings demonstrated a biphasic drug efflux mechanism for the formulations under studied. The first-two-hour release was fast, and then prolonged. occurred in the hours that followed. In comparison to pure TM, TM-BLs (BS1-BS6) released a greater amount of medicine throughout the trial. The pure TM discharged minimal medicine (19.36 ± 0.37 mg) from the dialysis bag due to its low solubility in water, with ranges of 42.61 ± 0.62% (BS3) to 74.39 ± 0.58% (BS2), which TM-BL release rate was significantly

https://doi.org/10.58985/jpam.2025.v03i02.33

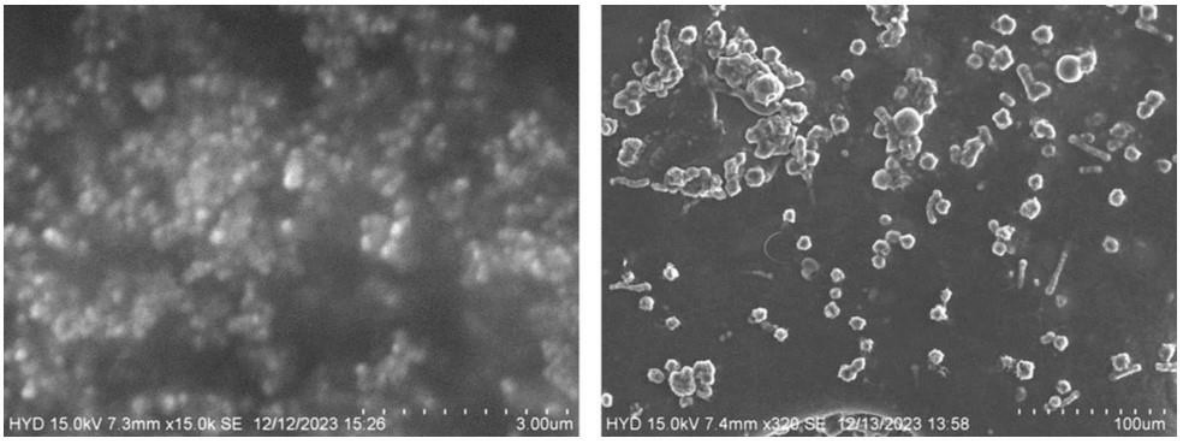

Figure 2. SEM images of Optimized TM-BLs (BS2) and TM-CBLs (CBS-1).

higher ($p < 0.05$). The extra medication release by TM was caused by bigger nano-metric vesicles and the availability of a higher effective surface area. An increase in the surface area results in additional drug-dissolution medium interaction sites [43].

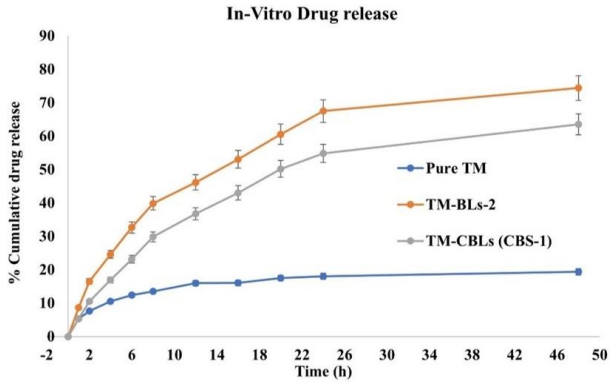

Figure 3. Release profiles of pure Trametinib (TM), TM-BLs (BS-2) and chitosan-coated TM-BLs (CBS-1). The data are shown as means ± SDs (n = 3).

The surfactant included in the BLs aided TM solubilization in the solvation medium. When TM was present on the vesicle surfaces, the release was fast at initially but slowed thereafter. Diffusion, carrier erosion, or swelling all contributed to the postponement of the drug release from the BLs' encapsulated medicine [44]. It was observed that TM-CBLs (CBS-1 and CBS-2) released their drugs at a slower rate than TM-BLs. In the final step of the study, TM-CBLs (CBS-1) significantly decreased release characteristics (56.34 ± 0.19 for 1% chitosan and 63.52 ± 0.85% for 0.5% chitosan; $p < 0.05$). Delaying release using an extra layer of chitosan might be helpful in increasing the duration of release throughout the body. The drug had to pass through two levels before reaching the release medium. Coating the negative surfaces of the BLs with chitosan inhibited TM release by electrostatic contact [45].

3.5. DPPH scavenging radicals in-vitro

The DPPH assay was used to determine the antioxidant capacities of pure TM-dispersion, TM-BLs and CBS-1 are shown in Fig. 4. As TM concentration increased, TM, TM-BLs, and TM-CBLs (CBS-1) antioxidant capacity decreased. Pure TM-dispersion exhibited antioxidant activity of 10.244-54.03% at concentrations of 5-200 µg/mL. However, at concentrations of 5 to 200 µg/mL TM-CBLs (CBS-1) and TM-BLs (22.87-96.13% and 18.67-85.06, respectively) demonstrated antioxidant activity. The findings revealed that, at all doses, TM-BLs displayed a considerably greater antioxidant capacity than pure TM, with a p-value less than.05. Pure QT had an activity of 54.03% at 200 µg/mL, whereas TM-BLs reached a high of 96.13% with a standard deviation of 1.36%. One possible explanation for the elevated TM activity in TM-BLs is that bile salts and CS increase TM solubility.

3.6. Scouring ABTS

Fig. 4 compares antioxidant activity of pure TM, TM-BLs, and TM-CBLs (CBS-1) using ABTS scavenging. TM antioxidant activity of the TM formulations was concentration-dependent manner. Pure TM showed 8.21-46.69% antioxidant activity at concentrations of 5-200 µg/mL. In TM-BLs and TM-CBLs (CBS-1) formulations, TM antioxidant activity ranged from 5 to 200 µg/mL, with 12.68-80.25% and 10.46-73.16 per milliliter, respectively. Compared to pure TM, TM-

https://doi.org/10.58985/jpam.2025.v03i02.33

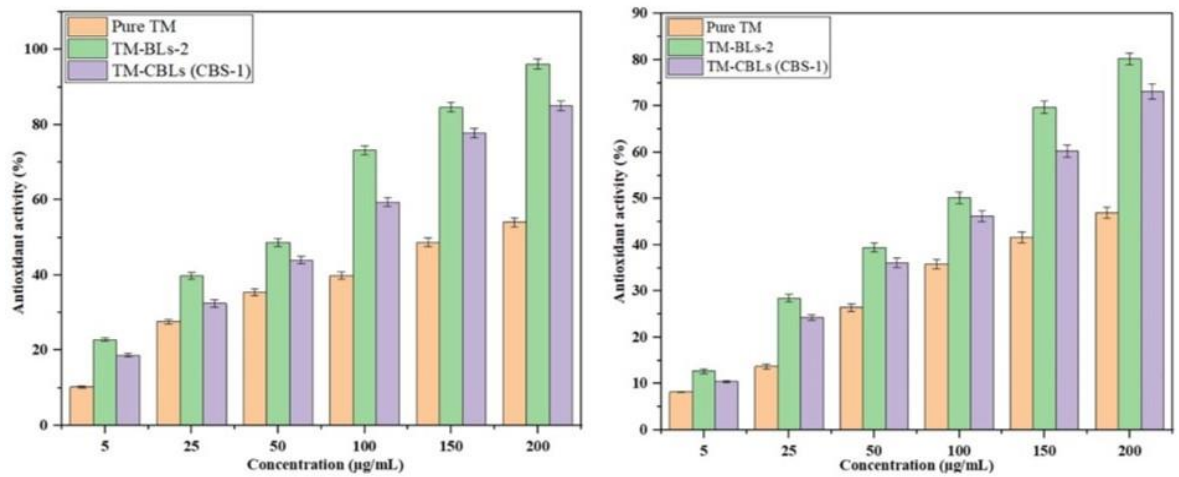

Figure 4. Antioxidant activity of DPPH radical and ABTS scavenging. of pure Trametinib (TM), TM-CBLs (BS-2), and TM-BLs (CBS-1) coated with chitosan in comparison to CBS-1. With n = 3, the values are given as the mean ± standard deviation. Both ** and *** showed that TM-BLs (CBS-1) had substantially different activity compared to pure TM, with p-values less than.01 and.001, respectively.

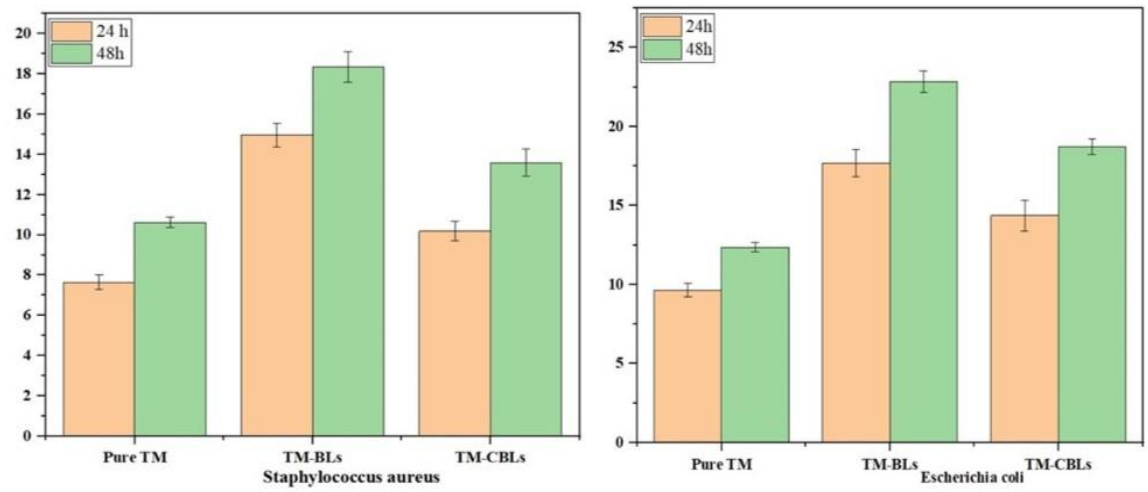

Figure 5. Analyzing the antimicrobial properties of pure TM, TM-BLs, and TM-CBLs (CBS-1) in relation to the zone of inhibition (ZOI) in terms of 24 and 48 hours respectively against Gram-positive and Gram-negative bacteria. Results indicate significant differences between TM-BLs and pure TM at $p < .01$ and $p < .001$, calculated as mean ± SD with n = 3.

BLs demonstrated significantly greater activity at all concentrations ($P < .05$). At 200/µg/mL, the TM exhibited a maximal activity of 46.89±1.18, 80.25 ± 1.24, and 73.16 ± 1.58% in its pure form, and 80.25 ± 1.24% in its TM-BLs form. Being more soluble in the nano-system, TM-BLs exhibited greater antioxidant activity compared to pure TM. The results demonstrated that compared to the DPPH technique, the ABTS approach had lower antioxidant activity.

3.7. Antibacterial activity

The antimicrobial evaluation of pure TM, TM-BLs and TM-CBLs (CBS-1) was done on S. aureus (Gram-positive) and E. coli (Gram-negative) microbial strains using the cup plate method for up to 48 h, and the results are shown in Fig. 5. TM was more susceptible to *E. coli* than *S. aureus* at the same concentration. The pure TM's 24-hour ZOI for *S. aureus* was 7.64 ± 0.56 mm, while for *E. coli* it was 9.64 ± 0.43 mm. In pure TM, the zone of inhibition (ZOI) for *S. aureus* and *E. coli* was 10.62 ± 0.26 mm and 12.37 ± 0.31 mm, respectively, after 48 h. Both the 24 and 48-hour tests showed that the TM-CBLs (CBS-1) and TM-BLs (CBS-1) formulations had significantly higher antibacterial activity against the investigated microorganisms

https://doi.org/10.58985/jpam.2025.v03i02.33

compared to pure TM ($P < .05$). Researchers discovered that the zone of inhibition (ZOI) for *S. aureus* was 14.97 ± 0.59, 10.18 ± 0.48 mm when using TM-BLs and TM-CBLs (CBS-1), respectively, while for *E. coli*, it was 17.69 ± 0.86 and 14.37 ± 0.98 mm. In contrast, TM-CBLs (CBS-1) and TM-BLs (CBS-1) exhibited far higher activity at 48 h, with MIC values of 18.35 ± 0.76 and 13.59 ± 0.67 mm against *S. aureus*, and 22.84 ± 0.69 and 18.72 ± 0.46 mm against *E. coli* respectively. Abdelbary et al. [1] found that TM-BLs have a high level of TM activity because the vesicles are nanosized, which increases the surface area available for diffusion. Sannasiddappa et al. [46] showed that surfactant and bile salt increase solubility and membrane permeability, improving activity. Since TM has a high permeability and is continuously released, covering it with chitosan to the BS formulation enhances its antibacterial action [47]. To exert its antibacterial effects, TM disrupts the cellular structures and membrane potential of Gram-positive and Gram-negative bacteria [48].

4. Conclusions

A combination of cholesterol, SDC, and Tween 80 was utilized in TM-BLs to varied degrees. The resulting vesicles were nanometric in size, with poor PDI, high EE and negative zeta potentials. The specific formulation (BS2) was then modified to enhance its mucoadhesion by adding chitosan (0.5-1% w/v). With a positive zeta potential, greater entrapment efficiency, and slower medicine delivery rate, the TM-CBLs coated with chitosan (CBS-1) and CBS-2 were somewhat larger. The mucoadhesion and TM permeability of the CBS-1 bilosomes that were coated with chitosan were significantly improved ($p < 0.05$). Both TM-BLs and TM-CBLs demonstrated more potent antibacterial action against *E. coli* and *S. aureus*, than TM-dispersion. According to the research, TM-BLs may be a viable option for improving TM effectiveness in treating specific diseases.

Authors' contributions

Conceptualization, A.K.C.; Data curation, C.S.; Investigation, A.S.; Methodology, C.S.; Project administration, writing – original draft, review and editing, C.S.

Acknowledgements

The Authors are thankful to the Deans of their respective Shri J.J.T.University, Rajasthan, for their support in carrying out this research.

Funding

Funding has been provided by Urmia University.

Availability of data and materials

All relevant data are within the paper and its supporting information files. Additional data will be made available on request according to the journal policy.

Conflicts of interest

Authors declare that there is no conflict of interest.

References

1. Abdelbary, A.A.; Abd-Elsalam, W.H.; Al-mahallawi, A.M. Fabrication of novel ultradeformable bilosomes for enhanced ocular delivery of terconazole: in vitro characterization, ex vivo permeation and in vivo safety assessment. Int. J. Pharm. 2016, 513, 688–696. https://doi.org/10.1016/j.ijpharm.2016.10.006
2. Shukla, A.; Mishra, V.; Kesharwani, P. Bilosomes in the context of oral immunization: development, challenges and opportunities. Drug Discov. Today. 2016, 21, 888–899. https://doi.org/10.1016/j.drudis.2016.03.013
3. Conacher, M.; Alexander, J.; Brewer, J.M. Oral Immunisation with peptide and protein antigens by formulation in lipid vesicles incorporating bile salts (Bilosomes). Vaccine. 2001, 19, 2965–2974. https://doi.org/10.1016/S0264-410X(00)00537-5
4. Wilkhu, J.S.; McNeil, S.E.; Anderson, D.E.; Perrie, Y. Characterization and optimization of bilosomes for oral vaccine delivery. J. Drug Target. 2013, 21, 291–299. https://doi.org/10.3109/1061186X.2012.747528
5. Pavlović, N.; Goločorbin-Kon, S.; Đanić, M.; Stanimirov, B.; Al-Salami, H.; Stankov, K.; Mikov, M. Bile acids and their derivatives as potential modifiers of drug release and pharmacokinetic profiles. Front Pharmacol. 2018, 9, https://doi.org/10.3389/fphar.2018.01283
6. Niu, M.; Lu, Y.; Hovgaard, L.; Guan, P.; Tan, Y.; Lian, R.; Qi, J.; Wu, W. Hypoglycemic activity and oral bioavailability of insulin-loaded liposomes containing bile salts in rats: The effect of cholate type, particle size and administered dose. Eur. J. Pharm. Biopharm. 2012, 81, 265–272. https://doi.org/10.1016/j.ejpb.2012.02.009
7. Aburahma, M.H. Bile salts-containing vesicles: Promising pharmaceutical carriers for oral delivery of

poorly water-soluble drugs and peptide/protein-based therapeutics or vaccines. Drug Deliv. 2014, 1–21. https://doi.org/10.3109/10717544.2014.976892

8. Kumar, G.P.; Rajeshwarrao, P. Nonionic surfactant vesicular systems for effective drug delivery—an overview. Acta Pharm. Sin. B. 2011, 1, 208–219. https://doi.org/10.1016/j.apsb.2011.09.002
9. Uchegbu, I.F.; Vyas, S.P. Non-ionic surfactant based vesicles (Niosomes) in drug delivery. Int. J. Pharm. 1998, 172, 33–70. https://doi.org/10.1016/S0378-5173(98)00169-0
10. Ruckmani, K.; Sankar, V. Formulation and optimization of zidovudine niosomes. AAPS Pharm. Sci. Tech. 2010, 11, 1119–1127. https://doi.org/10.1208/s12249-010-9480-2
11. Ahmad, J.; Singhal, M.; Amin, S.; Rizwanullah, Md.; Akhter, S.; Kamal, M.A.; Haider, N.; Midoux, P.; Pichon, C. Bile salt stabilized vesicles (Bilosomes): A novel nano-pharmaceutical design for oral delivery of proteins and peptides. Curr. Pharm. Des. 2017, 23, 1575–1588. https://doi.org/10.2174/1381612823666170124111142
12. Joseph, R.; Swaika, A.; Crozier, J.A. Vemurafenib: An evidence-based review of its clinical utility in the treatment of metastatic melanoma. Drug Des. Devel. Ther. 2014, 775. https://doi.org/10.2147/DDDT.S31143
13. Chen, J.; Fang, C.; Chang, C.; Wang, K.; Jin, H.; Xu, T.; Hu, J.; Wu, W.; Shen, E.; Zhang, K. Ultrasound-propelled liposome circumvention and SiRNA silencing reverse braf mutation-arised cancer resistance to trametinib. coll. Surf. B Biointerfaces. 2024, 234, 113710. https://doi.org/10.1016/j.colsurfb.2023.113710
14. Lee, J.W.; Choi, J.; Choi, Y.; Kim, K.; Yang, Y.; Kim, S.H.; Yoon, H.Y.; Kwon, I.C. Molecularly engineered SiRNA conjugates for tumor-targeted RNAi therapy. J. Contr. Rel. 2022, 351, 713–726. https://doi.org/10.1016/j.jconrel.2022.09.040
15. Li, W.; Zhang, H.; Assaraf, Y.G.; Zhao, K.; Xu, X.; Xie, J.; Yang, D.-H.; Chen, Z.-S. Overcoming ABC transporter-mediated multidrug resistance: molecular mechanisms and novel therapeutic drug strategies. Drug Resist. Updat. 2016, *27*, 14–29. https://doi.org/10.1016/j.drup.2016.05.001
16. Mas, C.; Boda, B.; CaulFuty, M.; Huang, S.; Wiszniewski, L.; Constant, S. Antitumour efficacy of the selumetinib and trametinib mek inhibitors in a combined human airway–tumour–stroma lung cancer model. J Biotechnol. 2015, 205, 111–119. https://doi.org/10.1016/j.jbiotec.2015.01.012
17. Tan, E.Y.; Pazdirkova, M.; Taylor, A.J.; Singh, N.; Iyer, G.R. Evaluation of a low-fat low-calorie meal on the relative bioavailability of trametinib and dabrafenib: Results from a randomized, open-label, 2-part study in healthy participants. clin. Pharmacol. Drug Dev. 2023, 12, 333–342. https://doi.org/10.1002/cpdd.1220
18. Djekic, L.; Janković, J.; Rašković, A.; Primorac, M. Semisolid self-microemulsifying drug delivery systems (SMEDDSs): Effects on pharmacokinetics of acyclovir in rats. Eur. J. Pharm. Sci. 2018, 121, 287–292. https://doi.org/10.1016/j.ejps.2018.06.005
19. Bramwell, V.W.; Perrie, Y. Particulate delivery systems for vaccines: what can we expect? J. Pharm. Pharmacol. 2006, 58, 717–728. https://doi.org/10.1211/jpp.58.6.0002
20. Wilkhu, J.S.; McNeil, S.E.; Anderson, D.E.; Perrie, Y. Characterization and optimization of bilosomes for oral vaccine delivery. J. Drug Target. 2013, 21, 291–299. https://doi.org/10.3109/1061186X.2012.747528
21. Zarenezhad, E.; Marzi, M.; Abdulabbas, H.T.; Jasim, S.A.; Kouhpayeh, S.A.; Barbaresi, S.; Ahmadi, S.; Ghasemian, A. Bilosomes as nanocarriers for the drug and vaccine delivery against gastrointestinal infections: Opportunities and challenges. J. Func. Biomat. 2023, 14, 453. https://doi.org/10.3390/jfb14090453
22. Waglewska, E.; Pucek-Kaczmarek, A.; Bazylińska, U. Novel surface-modified bilosomes as functional and biocompatible nanocarriers of hybrid compounds. Nanomaterials. 2020, 10, 2472. https://doi.org/10.3390/nano10122472
23. Zarenezhad, E.; Marzi, M.; Abdulabbas, H.T.; Jasim, S.A.; Kouhpayeh, S.A.; Barbaresi, S.; Ahmadi, S.; Ghasemian, A. Bilosomes as nanocarriers for the drug and vaccine delivery against gastrointestinal infections: Opportunities and challenges. J Func. Biomat. 2023, 14, 453. https://doi.org/10.3390/jfb14090453
24. Amarachinta, P.R.; Sharma, G.; Samed, N.; Chettupalli, A.K.; Alle, M.; Kim, J.C. Central composite design for the development of carvedilol-loaded transdermal ethosomal hydrogel for extended and enhanced anti-hypertensive effect. J. Nanobiotechnol. 2021, 19, 100. https://doi.org/10.1186/s12951-021-00833-4
25. Awan, A.M.; Farid, A.; Shah, S.U.; Khan, D.; Ur Rehman, F.; Dar, M.J.; Iftikhar, T.; Ghazanfar, S.; Galanakis, C.M.; Alamri, A.S.; et al. Nanocrytals-mediated oral drug delivery: Enhanced bioavailability of amiodarone. Pharmaceutics. 2022, 14, 1300. https://doi.org/10.3390/pharmaceutics14061300
26. Yusufkhan, P.S.; Deshmukh, S.R.; Farooqui, M. Design, synthesis, and biological evaluation of some methyl 2-(1H-pyrazol-4-ylthio)-1,2,3,4-tetrahydro-6-methylpyrimidine-5-carboxylate derivatives as potential DHFR inhibitors. Int. J. Health Sci. (Qassim). 2022, 6, 1018–1040. https://doi.org/10.53730/ijhs.v6nS1.4853

https://doi.org/10.58985/jpam.2025.v03i02.33

27. Jahangir, M.A.; Anand, C.; Muheem, A.; Gilani, S.J.; Taleuzzaman, M.; Zafar, A.; Jafar, M.; Verma, S.; Barkat, Md.A. Nano phytomedicine based delivery system for CNS disease. Curr. Drug Metabol. 2020, 21, 661–673. https://doi.org/10.2174/1389200221666200523161003
28. Singla, R.K.; De, R.; Efferth, T.; Mezzetti, B.; Sahab Uddin, Md.; Sanusi; Ntie-Kang, F.; Wang, D.; Schultz, F.; Kharat, K.R.; et al. The international natural product sciences taskforce (INPST) and the power of twitter networking exemplified through #INPST hashtag analysis. Phytomed. 2023, 108, 154520. https://doi.org/10.1016/j.phymed.2022.154520
29. Chaves, J.O.; de Souza, M.C.; da Silva, L.C.; Lachos-Perez, D.; Torres-Mayanga, P.C.; Machado, A.P. da F.; Forster-Carneiro, T.; Vázquez-Espinosa, M.; González-de-Peredo, A.V.; Barbero, G.F.; et al. Extraction of flavonoids from natural sources using modern techniques. Front Chem. 2020, 8. https://doi.org/10.3389/fchem.2020.507887
30. Chettupalli, A.K.; Ananthula, M.; Amarachinta, P.R.; Bakshi, V.; Yata, V.K. Design, formulation, in-vitro and ex-vivo evaluation of atazanavir loaded cubosomal gel. Biointerface Res. Appl. Chem. 2020, 11, 12037–12054. https://doi.org/10.33263/BRIAC114.1203712054
31. Unnisa, A.; Chettupalli, A.K.; Al Hagbani, T.; Khalid, M.; Jandrajupalli, S.B.; Chandolu, S.; Hussain, T. Development of dapagliflozin solid lipid nanoparticles as a novel carrier for oral delivery: Statistical design, optimization, in-vitro and in-vivo characterization, and evaluation. Pharmaceuticals. 2022, 15, 568. https://doi.org/10.3390/ph15050568
32. Shwetha, B.; Sudhanva, M.S.; Jagadeesha, G.S.; Thimmegowda, N.R.; Hamse, V.K.; Sridhar, B.T.; Thimmaiah, K.N.; Ananda Kumar, C.S.; Shobith, R.; Rangappa, K.S. Furan-2-carboxamide derivative, a novel microtubule stabilizing agent induces mitotic arrest and potentiates apoptosis in cancer cells. Bioorg Chem. 2021, 108, 104586. https://doi.org/10.1016/j.bioorg.2020.104586
33. Unnisa, A.; Chettupalli, A.K.; Hussain, T.; Kamal, M.A. Recent advances in epidermal growth factor receptor inhibitors (EGFRIs) and their role in the treatment of cancer: A review. Anticancer Agents Med. Chem. 2022, 22, 3370–3381. https://doi.org/10.2174/1871520622666220408090541
34. Bakshi, V.; Amarachinta, P.R.; Chettupalli, A.K. Design, development and optimization of solid lipid nanoparticles of rizatriptan for intranasal delivery: In vitro & in vivo assessment. Mater. Today Proc. 2022, 66, 2342–2357. https://doi.org/10.1016/j.matpr.2022.06.329
35. Jahangir, M.A.; Jain, P.; Verma, R.; Taleuzzaman, M.; Ahsan, M.J.; Chettupalli, A.K.; Muheem, A.; Mirza, M.A. Transdermal nutraceuticals delivery system for CNS disease. CNS Neurol Disord. Drug Targets. 2022, 21, 977–993. https://doi.org/10.2174/1871527321666220112154051
36. Jahangir, M.A.; Muheem, A.; Anand, C.; Imam, S.S. Traditional and modern applications of honey: An insight. In Therapeutic Applications of Honey and its Phytochemicals. Springer Singapore: Singapore, pp.151–169, 2020.
37. Chettupalli, A.K.; Rao, P.A.; Kuchukuntla, M.; Bakshi, V. Development and optimization of aripiprazole ODT by using box-behnken design. Res. J. Pharm. Technol. 2020, 13, 6195–6201. https://doi.org/10.5958/0974-360X.2020.01080.X
38. Prasad, R.R.; Kumar, J.R.; Vasudha, B.; Kumar, C.A. Formulation development and evaluation of allopurinol solid dispersions by solvent evaporation technique. Int. J. Appl. Pharm. 2018, 10, 168. https://doi.org/10.22159/ijap.2018v10i4.25311
39. Chettupalli, A.K.; Bukke, S.P.N.; Udom, G.J.; Saraswathi, T.S.; Rahaman, S.A.; Rai, S.N.; Kavitha, M.; Boggula, N.; Goruntla, N.; Yadesa, T.M.; et al. Investigating new bilosomes for ex vivo skin deposition, in vitro characterization, and transdermal delivery of nimodipine. Nanoscale Adv. 2024. https://doi.org/10.1039/D4NA00510D
40. Chettupalli, A.K.; Amara, R.R.; Amarachinta, P.R.; Ram Mohan Manda, R.M.; Garige,B.S.R.; Yata, V.K.; Formulation and evaluation of poly herbal liqui-solid compact for its anti-inflammatory effect. Biointerface Res. Appl. Chem. 2021, 12, 3883–3899. https://doi.org/10.33263/BRIAC123.38833899
41. Unnisa, A.; Chettupalli, A.K.; Alazragi, R.S.; Alelwani, W.; Bannunah, A.M.; Barnawi, J.; Amarachinta, P.R.; Jandrajupalli, S.B.; Elamine, B.A.; Mohamed, O.A.; et al. Nanostructured lipid carriers to enhance the bioavailability and solubility of ranolazine: Statistical optimization and pharmacological evaluations. Pharmaceuticals. 2023, 16, 1151. https://doi.org/10.3390/ph16081151
42. Rao A.P.; Chettupalli, A.K.; Chauhan, V.; Jadi, R.K. Design, formulation, in-vitro and in-vivo pharmacokinetic evaluation of nicardipine-nanostructured lipid carrier for transdermal drug delivery system. Mater Today Proc. 2023. https://doi.org/10.1016/j.matpr.2023.06.282
43. Sharaff, C.S.; Renukuntla, P.; Peddapalli, H.; Kuchukuntla, M.; Bakshi, V.; Jadi, R.K. Formulation, Development, and characterization of loratadine emulgel. J. Appl. Pharm. Res. 2024, 12, 42–50. https://doi.org/10.18231/j.joapr.2024.12.2.42.50

44. Unnisa, A.; Chettupalli, A.K. Promising role of phytochemicals in the prevention and treatment of cancer. Anticancer Agents Med. Chem. 2022, *22*, 3382–3400. https://doi.org/10.2174/1871520622666220425133936
45. Chettupalli, A.K.; Ajmera, S.; Amarachinta, P.R.; Manda, R.M.; Jadi, R.K. Quality by design approach for preparation, characterization, and statistical optimization of naproxen sodium-loaded ethosomes via transdermal route. Curr. Bioact. Comp. 2023, 19. https://doi.org/10.2174/1573407219666230606142116
46. Sannasiddappa, T.H.; Lund, P.A.; Clarke, S.R. In vitro antibacterial activity of unconjugated and conjugated bile salts on *Staphylococcus aureus*. Front. Microbiol. 2017, 8. https://doi.org/10.3389/fmicb.2017.01581
47. Zhang, R.; Li, Q.; Yang, L.; Dwibedi, V.; Ge, Y.; Zhang, D.; Li, J.; Sun, T. The antibacterial activity and antibacterial mechanism of the tea polyphenol liposomes/lysozyme–chitosan gradual sustained release composite coating. Int. J. Food Sci. Technol. 2022, 57, 3691–3701. https://doi.org/10.1111/ijfs.15694
48. Wang, G.; Li, X.; Wang, Z. APD3: The antimicrobial peptide database as a tool for research and education. Nucleic Acids Res. 2016, 44, D1087–D1093. https://doi.org/10.1093/nar/gkv1278

https://doi.org/10.58985/jpam.2025.v03i02.33